Int J Energy Environ Eng (2014) 5:72
DOI 10.1007/s40095-014-0072-x

ORIGINAL RESEARCH

Assessment of a practical model to estimate the cell temperature of a photovoltaic module

Rodolfo Araneo · Umberto Grasselli · Salvatore Celozzi

Received: 18 September 2013 / Accepted: 10 December 2013 / Published online: 12 March 2014

Abstract Instantaneous solar irradiance profiles or solar irradiation data collected with small time intervals (e.g., minutes) are usually required for the energy simulation of photovoltaic systems, especially as concerns the estimation of the cell temperature. However, meteorological stations and technical standards often provide just monthly average values of the horizontal daily solar irradiation; extensive climate databases that make available up to date hourly observation data or satellite-derived data are seldom available. The goal of the present paper is to investigate the suitability and the accuracy of a methodology aimed at estimating the time profile of the cell temperature of a photovoltaic system on the basis of only the monthly mean values of the daily global irradiation on a horizontal surface. The methodology consists of a chain of well-established models that are applied one after another, in a step-by-step procedure, in order to derive the cell temperatures from the solar radiation data. In particular, we selected different models as possible candidates for each step of the methodology and compared their predictions with measured data to identify the most suitable ones. In addition, we tried several combinations of models in order to identify the most accurate combination. Comparisons with data measured in Rome confirm the suitability of the proposed approach and give information about its accuracy.

R. Araneo (✉) · U. Grasselli · S. Celozzi
D.I.A.E.E. – Electrical Engineering Division, "Sapienza" University of Rome, Via Eudossiana 18, 00184 Rome, Italy
e-mail: rodolfo.araneo@uniroma1.it

U. Grasselli
e-mail: umberto.grasselli@uniroma1.it

S. Celozzi
e-mail: salvatore.celozzi@uniroma1.it

Keywords Photovoltaic cell · Irradiation · Irradiance · Linear model · Transient cell temperature

Introduction

In the last century, it has become clear worldwide the key role that energy plays in human life [1, 2]: It is at the base of our modern life and economy. Currently, the growing attention significance to environmental issues has stimulated countries to exploit renewable energy resources and to encourage their use [3–6]. Among them, solar photovoltaic (PV) energy is considered one of the leading potential sources of electricity for the twenty-first century [7–11]: It utilizes an abundant energy source (the sun), has no emissions, can be easily integrated in buildings, and the cost of the installed kWp is decreasing and becoming more and more affordable with payback periods shorter and shorter. In fact, in the recent years, the generation of solar electricity from PV systems has penetrated the energy market in those countries where clear and stable policy for subsidies have been made.

The rapid growth of the solar industry has expanded the importance of PV system design and application for more reliable and efficient operation [12, 13]. The design of PV systems in an economically optimal way [14–16] is usually done through detailed computer simulations [17, 18]: Transient analysis is useful when the different energy phenomena that take place in the heart of the production systems [19] should be accounted for, e.g., if they present some kind of solar tracking [20].

In performing such an analysis, the accurate evaluation of the operating temperature of the PV device (either a simple module or a PV/thermal collector of a building-integrated PV array) is of paramount importance [21], because several performance parameters of the PV system

depend on it through the so-called temperature coefficients [22]. The derivatives can be determined for short-circuit current (I_{sc}), maximum power current (I_{mp}), open-circuit voltage (V_{oc}), maximum power voltage (V_{mp}), and maximum power (P_{mp}), as well as fill factor (FF) and, finally, efficiency (η). Particular attention is focused on the energy conversion factor of a PV system that is commonly described by the electrical efficiency η [23] defined as the ratio of the electricity generated to the global solar irradiation impinging on the collector' surface. Furthermore, the temperature coefficients for PV systems are directly related to the temperature coefficients for their individual cells, and thus, the so-called cell temperature T_c is the real key parameter to be identified because it affects, directly or indirectly, the energy conversion efficiency [24] of any PV system. In addition, it plays an important role in PV system design and sizing, since often the worst case operating conditions dictate the array size.

More physical insights into the dependence of the electric energy conversion mechanisms on the cell temperature can be obtained looking at the solid state physics of the cell [25–27]: The energy bandgap of semiconductors, and consequently the quantum conversion efficiency, tends to decrease as the temperature increases [24, 28] due to the fact that the interatomic spacing increases when the amplitude of the atomic vibrations increases as a consequence of the increased thermal energy. An increased interatomic spacing decreases the potential seen by the electrons in the material, which in turn reduces the size of the energy bandgap (a direct increase/decrease in the interatomic distance, and consequently, bandgap, can be obtained also by applying high compressive/tensile stress [29, 30]).

Despite its great importance, the cell temperature T_c depends on such a lot parameters and weather variables that its correct evaluation is the critical point of any methodology aimed at properly sizing PV systems. A scan of the relevant literature [31, 32] easily produces an impressive number of correlations expressing the cell temperature as a function of the pertinent weather variables, namely, ambient temperature, local wind speed as well as the solar irradiance on the surface of PV systems, which are tilted toward the sun to maximize the amount of the incident solar radiation [25, 26, 33]. Radiation data, such as hourly direct and diffuse irradiance on the tilted surface, were usually required but smaller time steps could be necessary when load profiles vary with smaller time constants. However, meteorological stations and national or international standards often provide only daily global irradiation data on horizontal surface (sometimes they measure also the diffuse component), which are commonly summarized in monthly average values [34–36].

In this framework, the objective of the present paper is a task of great practical importance from an engineering point of view: We want to define a methodology for estimating the operating cell temperature T_c starting *only* from the monthly mean value of the daily global irradiation on a horizontal surface. The methodology consists of a chain of models that are well-established in literature and that we apply in a step-by-step procedure to derive the cell temperature from the solar radiation data. In particular, we compare several models, focusing on how to couple them in order to obtain the best accuracy in the predicted data; finally, we investigate the suitability and the accuracy of the proposed methodology. In addition, we provide two new models for calculating the solar irradiance and the ambient temperature profiles. Comparisons with data measured in Rome confirm the applicability of the proposed approach and give information about the accuracy of the model.

The paper is organized as follows. In "Theory and models" section, the proposed procedure is illustrated: Subsection "Irradiance model" analyzes the radiation models used to predict the irradiance profiles on a tilted surface from the monthly average daily global irradiations on a horizontal surface; the models used to predict the PV cell temperature from the irradiance profiles are described in Subsection "Operating temperature of the photovoltaic cell." Section "Results and discussion" presents the relevant results: The measurement setup is described in Subsection "Setup," while in Subsection "Assessment of the models" a statistical analysis is performed on the results in order to assess the validity of the whole procedure, identifying and discussing the most accurate models. Finally, the main conclusions of the work are drawn.

Theory and models

The goal of the procedure described in the following subsections is to estimate the transient temperature of the photovoltaic cell during the day n_d of the year, placed on a surface S_T tilted γ_t with respect to the horizontal plane and rotated α_t with respect to the north–south direction, starting from the monthly average daily global irradiation value $\overline{H}$ on a horizontal surface (the configuration is illustrated in Fig. 1). The procedure consists of five steps that are applied one after another in succession as shown in Fig. 2. Each step is based on the application of well-established models that are compared and discussed in order to obtain an accurate and robust procedure.

Irradiance model

As is well-known, the quantity of solar radiation reaching the Earth's surface during a day is governed by several factors: the solar elevation at noon, the duration of the day, the turbidity of the air, the total amount of water vapor in

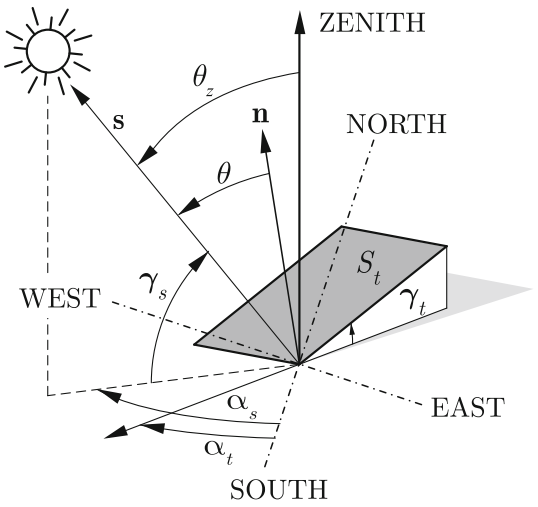

Fig. 1 Geometrical configuration of the PV cell placed on a surface S_T tilted γ_t from the horizontal plane and rotated α_t from the north–south direction

the air, and the type and amount of clouds [37]. When a direct measurement is not available, as often happens, H is taken as the monthly mean value $\overline{H}$ referred to the "average day" of the month, i.e., the day when the solar declination δ is equal to the average value of the month [33, 26]. The monthly average daily irradiation can be obtained from national standards or measurement campaigns or trough an Angstrom-type regression equation that relates the ratio between monthly average daily global irradiation and monthly average daily extraterrestrial irradiation at a particular location to the average fraction of possible sunshine hours [38].

From $\overline{H}$, the global hourly irradiation H_h on a horizontal surface during the day n_d of the month has to be somehow evaluated in order to compute the hourly global irradiation G_{Th} incident on S_T (for all the details see [33]), as

$$G_{Th} = B_{Th} + D_{Th} + R_{Th}, \tag{1}$$

where the direct B_{Th}, sky-diffuse D_{Th}, and ground reflected (albedo) R_{Th} components are given by

$$B_{Th} = B_h r_b = (1 - k_d) r_b H_h \tag{2a}$$

$$D_{Th} = D_h r_d = k_d r_d H_h \tag{2b}$$

$$R_{Th} = \rho \frac{1 - \cos \gamma_t}{2} H_h. \tag{2c}$$

In Eq. (2) B_h, D_h, and $H_h = B_h + D_h$ are, respectively, the direct, diffuse, and global hourly irradiation on a horizontal surface, $r_b = \cos\theta / \cos\theta_z$ is the beam radiation factor, with θ the solar incidence angle on S_T, and θ_z the zenith angle of the Sun [33, chap. 1], k_d is the cloudiness index, $r_d = D_{Th}/D_h$ is the conversion factor for the hourly diffuse irradiation, and ρ is the ground reflectivity. It is assumed that the ground has very low reflectance, i.e., the reflected component is much lower than the sum of the direct and diffuse irradiation, so that an isotropic model may be used for the computation of the ground albedo. The relevant parameters in Eq. (2), i.e., H_h, k_d and r_d, are evaluated as described in the following Subsections "Horizontal hourly global irradiation values," "Hourly diffuse and direct irradiation," and "Hourly diffuse irradiation on a tilted surface," respectively.

Once the hourly global irradiation G_{Th} is known, the irradiance profile $I_{gT}(t)$ on the tilted surface is finally computed as reported in Subsection "Solar irradiance profiles".

Horizontal hourly global irradiation values

Several well-established methods have been proposed in literature to convert the average daily horizontal global irradiation H into horizontal hourly global values H_h. Most of them assume the day is symmetric, i.e., with same irradiation values for hours situated symmetrically with

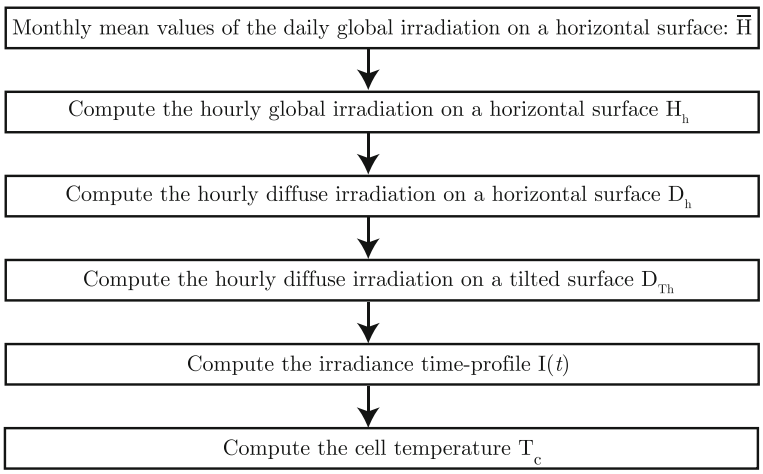

Fig. 2 Steps of the proposed procedure

respect to the solar noon [39–41], while a few of them try to account for the asymmetries between morning and afternoon [42, 43]. The characterization of a general distribution of hourly solar irradiation is made difficult by the non-stationary nature of the solar irradiation, which is affected by an unpredictable noise due to a variety of factors. Recently, sophisticated methods have been proposed, such as neural networks and autoregressive average models [44, 45]. Though all these methods are reliable and show good accuracy, they make the formulation more difficult to be implemented, so that the simple but effective correlation model presented in [41] is used. The correlation has been confirmed to be compatible with results obtained for Canada, India, Israel, and, lastly, Corsica [46] and to work best for clear days, when solar processes produce most of the output. According to this model, the hourly values H_h are computed as:

$$H_h = r_t \overline{H}, \tag{3}$$

where the ratio r_t is given by

$$r_t = \frac{1}{2}\left(a + b\cos\frac{\omega_2+\omega_1}{2}\right) \cdot \frac{(\sin\omega_2 - \sin\omega_1) - \frac{\pi(\omega_2-\omega_1)}{180^\circ}\cos\omega_s}{\sin\omega_s - \frac{\pi\omega_s}{180^\circ}\cos\omega_s} \tag{4}$$

with

$$a = 0.4090 + 0.5016\sin(\omega_s - 60^\circ) \tag{5a}$$

$$b = 0.6609 - 0.4767\sin(\omega_s - 60^\circ). \tag{5b}$$

In (4), ω_1 and ω_2 are the hour angles at the beginning and end, respectively, of the hour in question ($\omega = 15^\circ(12-h)$, with h the solar time), and ω_s is the sunset hour angle for the day equal to $\cos^{-1}(-\tan\delta\tan\phi)$, with ϕ latitude of the location and δ declination for the day, which can be computed by means of the Cooper's or Spencer's formulas [33, chap. 1].

In (3), the monthly mean value $\overline{H}$ of the global daily solar irradiation on a horizontal surface has been used and the coefficient r_t accounts for the specific day n_d of the month through the declination angle δ. The suitability and accuracy of (3) in the framework of the whole proposed methodology has been assessed in Section "Results and discussion."

Hourly diffuse and direct irradiation

Since the pioneer work of Liu and Jordan [39] in the early 1960s, several models have been proposed in literature to evaluate the hourly average cloudiness index $k_d = D_h/H_h$, where D_h is the hourly sky-diffuse irradiation on a horizontal surface. A complete list of these models is beyond the scope of the present paper; comparative studies among the most frequently used correlations can be found in [47–49]. These correlations are usually expressed in terms of first- to fourth-degree polynomials relating the diffuse fraction k_d with the hourly clearness index $k_t = H_h/H_{0h}$, defined as the ratio of the hourly global solar irradiation H_h and the hourly extraterrestrial solar irradiation on a horizontal surface H_{0h} [33, chap. 1].

In the present work, we have compared the four models from Karatasou [50], Erbs [51], Miguel [52], and Reindl [53] against experimental irradiation values for the Italian location of Rome over a period of 2 years.

Karatasou [50] model is a third-order polynomial correlation based on data from one location at Athens (Greece):

$$\begin{aligned} k_d &= 0.9995 - 0.05k_t - 2.415k_t^2 + 1.4926k_t^3 && k_t \le 0.78 \\ k_d &= 0.20 && k_t > 0.78. \end{aligned} \tag{6}$$

Erbs [51] model is a fourth-order polynomial correlation based on data from four locations in USA:

$$\begin{aligned} k_d &= 0.9996 - 0.09k_t && k_t \le 0.22 \\ k_d &= 0.951 - 0.1604k_t + 4.388k_t^2 \\ &\quad -16.638k_t^3 + 12.336k_t^4 && 0.22 < k_t \le 0.80 \\ k_d &= 0.1652 && k_t > 0.80. \end{aligned} \tag{7}$$

Miguel [52] model yields a third-order polynomial for k_d using a data set from several sites in the north Mediterranean Belt (e.g., France, Greece, Italy, Portugal, and Spain):

$$\begin{aligned} k_d &= 0.9943 - 0.081k_t && k_t \le 0.21 \\ k_d &= 0.724 + 2.734k_t - 8.32k_t^2 + 4.967k_t^3 && 0.21 < k_t \le 0.76 \\ k_d &= 0.1766 && k_t > 0.76. \end{aligned} \tag{8}$$

Finally, Reindl [53] established a very simple correlation, studying the influence of climatic and geometric variables on the hourly diffuse fraction based on data measured at five European and US locations:

$$\begin{aligned} k_d &= 1.0234 - 0.248k_t && k_t \le 0.30 \\ k_d &= 1.45 - 1.67k_t && 0.3 < k_t \le 0.78 \\ k_d &= 0.1474 && k_t \ge 0.78. \end{aligned} \tag{9}$$

A comparative analysis of the predictions of the four models based on consolidated standard statistical parameters [54] reported in Section "Results and discussion," has showed that the physically based method proposed by Miguel correlates better with the data collected in Rome.

Once the hourly diffuse irradiation component D_h is known, the hourly direct irradiation B_h is then computed as $B_h = H_h - D_h$.

Hourly diffuse irradiation on a tilted surface

The conversion of the hourly horizontal diffuse irradiation D_h to hourly diffuse irradiation D_{Th} on the tilted surface S_T can be expressed as

$$D_{Th} = r_d D_h, \tag{10}$$

where r_d is the conversion factor.

The methods proposed in literature for the evaluation of r_d are classified into isotropic or anisotropic models. The isotopic models assume that the sky dome irradiates uniformly so that the diffuse radiation incident on the tilted surface depends on the fraction of the sky dome seen by it. The anisotropic models try to model the anisotropy of the diffuse radiation, decomposing it in different components, i.e., the circumsolar component (Sun's aureole), the brightness of the horizon, and the isotropic component of the sky dome. Validation studies and testing of several well-established models to predict r_d have been performed in [55–57]. However, results are not always in agreement, and ranking these models according to their accuracy is not simple. In fact, their abilities to predict the diffuse radiation on a tilted surface are a priori function of the atmospheric conditions (clear, partially cloudy, or overcast sky), since they take assumptions about the isotropy or anisotropy of the sky dome. The way in which the anisotropy is accounted for makes them strongly dependent on the surface orientation (it has been observed that all models produce large errors for east–west-facing PV surfaces [55]). In addition, several models are based on empirical data obtained for some particular geographical locations, so that they show enhanced/poor accuracy when used in locations with similar/different irradiation conditions. Anyway, the use of well-known statistical indicators [54], and much more complex statistical analyses [56] performed on data collected from several locations in the world, have generally, but not always, indicated that the Ma-Iqbal [58], Reindl [59], Muneer [60], and Perez [61, 62] models are those that give the most accurate predictions for small azimuthal angle α_t (i.e., south-facing surfaces). In addition, in [56] it was found that the Ma-Iqbal model performs best under all sky conditions, clear and partially cloudily, whereas the Muneer model gives the best results for cloudy-sky conditions.

In this framework, we have selected these four models and compared their predictions against experimental irradiation values, as reported in Section "Results and discussion."

In the model proposed by Ma-Iqbal [58], the diffuse irradiance on an inclined plane is considered to be the addition of the circumsolar component coming from the direction near the solar disk and a diffuse component isotropically distributed from the rest of the sky. These two components are weighted according to an index of anisotropy that represents the transmittance through the atmosphere of direct irradiance. Unlike the original model of Hay [63] who defined his own sky-clarity factor $F = B_h/H_{0h}$, Ma and Iqbal used the clearness index k_t as index of anisotropy. According to the Ma-Iqbal model, the conversion factor r_d can be computed as

$$r_d = k_t r_b + (1 - k_t)\frac{1 + \cos\gamma_t}{2}. \tag{11}$$

The Reindl model [59] assumes linearity of the isotropic and circumsolar contributions to the diffuse radiation on a tilted plane according to the Hay model and adopts the same correction factor that takes into account the brightness of the sky near the horizon used in the Temps-Coulson model [64]. The conversion factor r_d is determined as:

$$r_d = F r_b + (1 - F)\frac{1 + \cos\gamma_t}{2}\left[1 + \sqrt{\frac{B_h}{H_h}}\sin^3\frac{\gamma_t}{2}\right], \tag{12}$$

where $F = B_h/H_{0h}$ is the Hay's sky-clarity factor.

Muneer [60], partially following the model proposed by Gueymard [65], considers that the irradiance can be expressed as a linear combination of values between fully covered sky and cloudless sky which in turn is the addition of the circumsolar component and a hemispheric factor. The conversion factor r_d is expressed as:

$$r_d = T_M(1 - F_M) + F_M r_b, \tag{13}$$

where T_M is the Muneer's tilt factor defined as the ratio between the slope background diffuse radiation and the horizontal diffuse radiation given by

$$T_M = \frac{1 + \cos\gamma_t}{2} - \frac{2B}{3 + 2B}\left[\frac{\gamma_t\cos\gamma_t - \sin\gamma_t}{\pi} + \frac{1 - \cos\gamma_t}{2}\right], \tag{14}$$

and F_M is a composite anisotropic index, equal to Hay's sky-clarity factor F for non-overcast conditions and 0 for overcast sky. In Eq. (14), B is the radiation distribution index whose values depend on the particular sky and azimuthal conditions, and the location: for southern European locations, Muneer recommends the following correlation

$$\frac{2B}{3 + 2B} = \pi\left(0.00263 - 0.712F - 0.688F^2\right). \tag{15}$$

The Perez model is more computationally cumbersome than the others because it represents the isotropic diffuse, circumsolar, and horizon brightening components with more details using empirically derived coefficients. Yet, the model developed by Perez in [62] is considerably simpler, and more accurate, than the original model proposed in his first work [61]. In fact, the conversion factor r_d is computed as

$$r_d = (1 - F_1)\cos^2\left(\frac{\gamma_t}{2}\right) + r'_b F_1 + F_2 \sin\gamma_t. \quad (16)$$

where F_1 and F_2 are, respectively, the circumsolar and horizon brightness coefficients

$$F_1 = \max\left[0,\ \left(f_{11} + f_{12}\Delta + \frac{\pi\theta_z}{180} f_{13}\right)\right] \quad (17a)$$

$$F_2 = f_{21} + f_{22}\Delta + \frac{\pi\theta_z}{180} f_{23}, \quad (17b)$$

where θ_z is the beam radiation factor, $\Delta = k_d k_t$ is the brightness parameter and f_{ij} are tabulated statistically derived coefficients [62] depending on the clearness parameter

$$\varepsilon = \frac{1}{1 + 5.535 \cdot 10^{-6}\theta_z^3}\left(\frac{D_h + \frac{B_h}{\cos\theta_z}}{D_h} + 5.535 \cdot 10^{-6}\theta_z^3\right). \quad (18)$$

In Eq. (16), r'_b is the modified beam radiation conversion factor defined as

$$r'_b = \frac{\max(0, \cos\theta)}{\max(\cos 85^\circ, \cos\theta_z)}. \quad (19)$$

Solar irradiance profiles

The transient simulation of the temperature of photovoltaic modules requires the knowledge of continuous profiles versus time t of the global solar irradiance I_{gT} on the tilted surface during the day n_d. Starting from the hourly mean values of the global irradiation G_{Th}, various studies consider that the solar irradiance is distributed over the time with a constant repartition which, however, has been demonstrated to be an unrealistic hypothesis, since this assumption does not provide a precise idea of the different transient energy phenomena that take place in the heart of the solar system. In [17], it was proposed a linear model that allows the determination of irradiance data, averaged on small time step Δt (e.g., one minute), from hourly irradiation values. Starting from this work, a second order model is here proposed.

The solar irradiance $I_j(t)$, on the tilted surface, is assumed to vary in a quadratic manner between the beginning time h_{j-1} and the ending time h_j of the j-th hour of the day (e.g., the first hour begins at time t equal to $h_0 = 00{:}00$ and ends at time $h_1 = 01{:}00$), i.e.,

$$I_j = a_j t^2 + b_j t + c_j, \quad (20)$$

with $j = 1, 2 \ldots 24$ and $h_0 = 0$, $h_1 = 1$, $\ldots$ $h_{24} = 24$. It is evident that it is necessary to enforce three equations for every hour occurring between sunrise h_{SR} and sunset h_{SS} times since the number of unknowns for every hourly profile is equal to three. As shown in Fig. 3a, if sunrise or sunset does not occur in the j-th hour, the three conditions to be enforced are as follows:

- the integration of the irradiance $I_j(t)$ over the hour must be equal to the hourly irradiation H_j (on tilted or horizontal surface),

$$\int_{h_{j-1}}^{h_j} I_j(t)\mathrm{d}t = H_j; \quad (21)$$

- the profiles $I_j(t)$ and $I_{j+1}(t)$ and their first derivatives at every time h_j between two successive hours must be continuous

$$a_j h_j^2 + b_j h_j + c_j = a_{j+1} h_j^2 + b_{j+1} h_j + c_{j+1} \quad (22a)$$

$$2a_j h_j + b_j h_j = 2a_{j+1} h_j + b_{j+1} h_j. \quad (22b)$$

If sunrise or sunset occur in the considered j-th hour (Fig. 3b), Eq. (21) must be modified according to

$$\int_{h_{SR}}^{h_j} I_j(t)\mathrm{d}t = H_j \quad (23a)$$

$$\int_{h_{j-1}}^{h_{SS}} I_j(t)\mathrm{d}t = H_j, \quad (23b)$$

because the model considers that the solar irradiance has been spread over the hour whereas it just took place since sunrise or until sunset

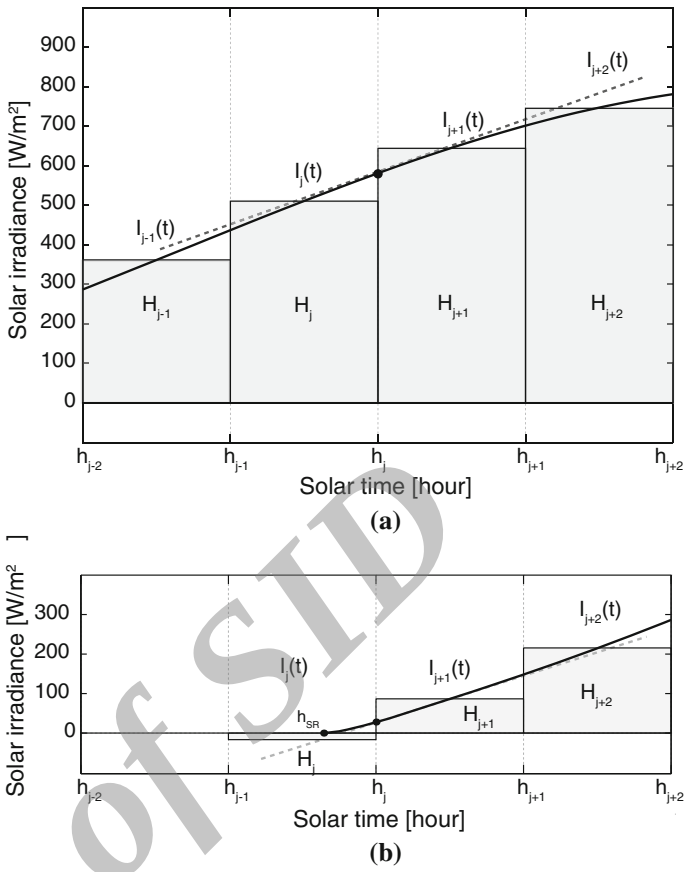

Fig. 3 Illustration of the quadratic model for approximating the solar irradiance profile from hourly mean values of the global irradiation: **a** daylight hours; **b** hour when sunrise takes place

Then, in the hour when sunrise (or sunset) takes place, the value of the irradiance profile at h_{SR} (or h_{SS}) must be set equal to zero, i.e., $I_j(t \leq h_{SR}) = 0$ (or $I_j(t \geq h_{SS}) = 0$).

Operating temperature of the photovoltaic cell

The cell operating temperature T_c is the proper temperature to use in order to predict the electrical performance of the PV module. Because of the internal processes that take place within the cells during their exposure to sun, a large portion of the incident irradiance is degraded and released as heat. Standard heat transfer mechanisms must be accounted for to compute the appropriate energy balance on the cell/module leading to the prediction of T_c. At steady-state conditions, only convection and radiation mechanisms are usually considered, since they are prevalent on the conduction mechanism that merely transports heat toward the surfaces of the mounting frame (especially in the case of rack-mounting free-standing arrays). A survey of the explicit and implicit correlations proposed in literature linking T_c with standard weather variables and material and system-dependent properties can be found in [32].

In the present work, we compare four different explicit equations against experimental data. Among the large number of correlations proposed in literature, we have chosen the equations whose application appears to be the best and simplest. Hence, we have chosen equations that are explicit, depend on easily measurable parameters and, are of wide applicability. The four alternative correlations are [31, 32, 66, 67]

$$T_c = T_a + \frac{I_{gT}}{I_{NOCT}}\left(T_{NOCT} - T_{a,NOCT}\right) \tag{24a}$$

$$T_c = T_a + \left(\frac{0.32}{8.91 + 2.0v_w}\right) I_{gT} \tag{24b}$$

$$T_c = 0.943T_a + 0.028I_{gT} - 1.528v_w + 4.3 \tag{24c}$$

$$T_c = T_a + 0.0138I_{gT}(1 + 0.031T_a)(1 - 0.042v_w) \tag{24d}$$

where T_{NOCT} is the so-called nominal operating cell temperature (the temperature T_{NOCT} is defined as the temperature of the cell at the conditions of the nominal terrestrial environment (NTE): Solar irradiance $I_{NOCT} =$ 800 W/m^2, ambient temperature $T_{a,\ NOCT} = 20$ °C, average wind speed 1 m/s, nil electrical load, and free-standing mounting frame oriented normal to solar noon), T_a is the ambient temperature and v_w is the wind speed

(free stream wind speed in the windward side of the PV array).

Two remarks are necessary before applying the previous expressions. The cell temperature T_c may be higher than the back-side temperature T_b, which is the directly measured quantity, of a few degrees, being this difference dependent mainly on the module substrate material and the intensity of the solar irradiance $I_{gT}(t)$. The two temperatures are related through the simple linear expression [68]

$$T_c = T_b + \frac{I_{gT}}{I_{ref}} \Delta T_{ref}, \tag{25}$$

where I_{ref} is the reference solar irradiance of 1,000 W/m^2 and ΔT_{ref} is the temperature difference under this reference solar irradiance. This temperature difference is typically ranging between 2 and 3 °C for flat-plate modules in an open-rack setting [68].

The evaluation of T_c requires an accurate estimation of the ambient temperature. Assuming it constant during the day and equal to the average value is an unrealistic assumption. Here the following third-order approximation for a smooth transient from the minimum T_{min} to the maximum T_{max} temperatures registered during the day is assumed

$$T_a(t) = \frac{1}{(h_{SR} - h_{SS})^3} \Big[(h_{SS} - t)^2 (h_{SR} - 3h_{SS} + 2t) T_{max} + (3h_{SR} - h_{SS} - 2t)(h_{SS} - t)^2 T_{min} \Big]. \tag{26}$$

It has been observed that the approximation (26) provides accurate agreement with the measured results during the hours from sunrise to sunset, when the PV system produces energy.

Results and discussion

The ability of the proposed procedure to predict the PV cell temperature is tested comparing the predicted results with experimental values measured in Rome during the two years 2010 and 2011. The four models selected for the computation of the cloudiness index k_d in Subsection "Hourly diffuse and direct irradiation," for the computation of the hourly diffuse irradiation on a tilted surface (i.e., the conversion factor r_d) in Subsection "Hourly diffuse irradiation on a tilted surface," and for the computation of the cell temperature T_c in Subsection "Operation temperature of the photovoltaic cell" are compared. Furthermore, we studied the best combination of these models in order to obtain the best accuracy of the predictions.

The accuracies have been assessed using well-known statistical indicators [54]: the mean bias error (MBE), the root mean square error (RMSE), and the coefficient of determination (R^2). They are defined as:

$$\mathrm{MBE} = \frac{1}{N} \sum_{i=1}^{N} x_{p,i} - y_{m,i} \tag{27a}$$

$$\mathrm{RMSE} = \sqrt{\frac{1}{N} \sum_{i=1}^{N} (x_{p,i} - y_{m,i})^2} \tag{27b}$$

$$\mathrm{R}^2 = \frac{\mathrm{ESS}}{\mathrm{TSS}} = \frac{\sum_{i=1}^{N} (x_{p,i} - \bar{y}_m)^2}{\sum_{i=1}^{N} (y_{m,i} - \bar{y}_m)^2}, \tag{27c}$$

where N is the number of data points during each day, x_p, i and y_m, i are, respectively, the predicted and measured (observed) data points, $\bar{y}_m = \sum_{i=1}^{N} y_{m,i}$ is the mean value of the measured data, ESS is the Explained Sum of Squares, and TSS is the Total Sum of Squares. The MBE determines whether the model underestimates or overestimates experimental data, the RMSE gives a measure of how well the model can predict the experimental data (it provides information on the short-term performance of the model by allowing a term-by-term comparison of the actual deviation between the estimated and the measured values), and R^2 provides a measure of how well the model explains observed phenomena (its value shows how well future outcomes can be predicted by the model).

Setup

The irradiance and temperature data have been measured on the roof of the Department of Electrical Engineering, Faulty of Engineering, located in Rome, Italy ($\phi = 41°53'38''$N, $\lambda = 12°29'37''$E) during the two years 2010 and 2011. As shown in Fig. 4a, the setup consists of 20 polycrystalline Si-modules mounted in free-standing manner, i.e., on racks placed above the roof. The modules are tilted $\gamma_t = 30°$ from the horizontal surface and are south-facing ($\alpha_t = 0°$). The modules are subdivided in two strings, each formed by the series connection of 10 modules (the upper and lower ones) which have been left open-circuited during the temperature measurements. The manufacturer's specifications give $T_{NOCT} = 48 \pm 3$ °C (fixed to 50 °C, in the following) and $\Delta T_{ref} = 2$ °C (added to T_b which is the real measured quantity). Figure 4b shows the PT100 sensors (platinum resistance thermometers sensors) placed on the back of the PV module to measure the rear temperature T_b. Six sensors have been placed on three modules (two sensors per module) in

order to investigate the uniformity of the temperature among different modules with the same exposition. An identical PT100 sensor has been used to measure the ambient temperature as shown in Fig. 4c. The Yokogawa DC100 data collector unit has been used to collect and register the data on seven independent channels. The solar irradiance data were acquired using class-1 pyranometer Delta-Ohm LP Pyra. The measurements have been performed with a real-time data-acquisition step of 30 sec (2880 data points for each channel per day). According to the Guide JCGM [69], the expanded uncertainty $U(T_c)$ with a coverage factor $k = 2$ (corresponding to a confidence level $p = 95.45$ %) is ± 0.81 °C.

The monthly average daily irradiation values used in the following computations are, {2.33, 3.28, 4.25, 5.29, 6.34, 6.74, 6.72, 5.87, 4.70, 3.61, 2.51, 2.12} kWh/(m^2 day), provided by national standards for the twelve months of the year, respectively. The albedo factor has been set equal to 0.2 (dark-colored, rough soil surfaces). No particular shading affected the PV system output.

Assessment of the models

As explained in the previous Section, the correct modeling of the irradiance incident on the tilted surface of the PV module is required at the first step of the proposed procedure. Hence, it is mandatory to assess the accuracy of the selected models used for its prediction.

The diffuse and direct irradiation values on a horizontal surface predicted by the four models used for the computation of the cloudiness index k_d (Subsection "Hourly diffuse and direct irradiation") are reported in Figs. 5 and 6, respectively, where they are plotted against observed values. The modeled results have been computed considering in input of Eq. 3 the aforementioned monthly average daily irradiation values $\overline{H}_h$ provided by national standards in order to compute the hourly values of the global irradiation on a horizontal surface and then decomposing these global values into diffuse and direct components. The figures also plot for each model the linear line of best fit (dotted line) as well as a line of one-to-one correlation

(a)

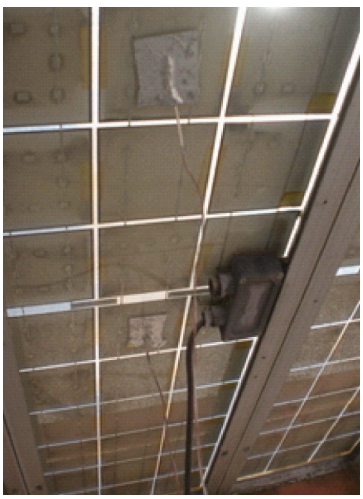

(b)

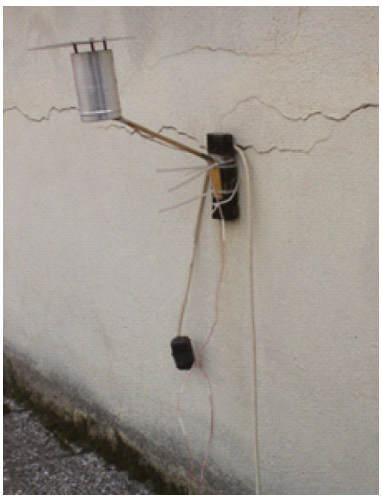

(c)

Fig. 4 Test setup consisting of: **a** free-standing modules placed on the roof of the Electrical Engineering Department; **b** PT100 sensors used to measure the back temperature T_b of the modules; **c** PT100 sensor for the measurement of the ambient temperature T_a

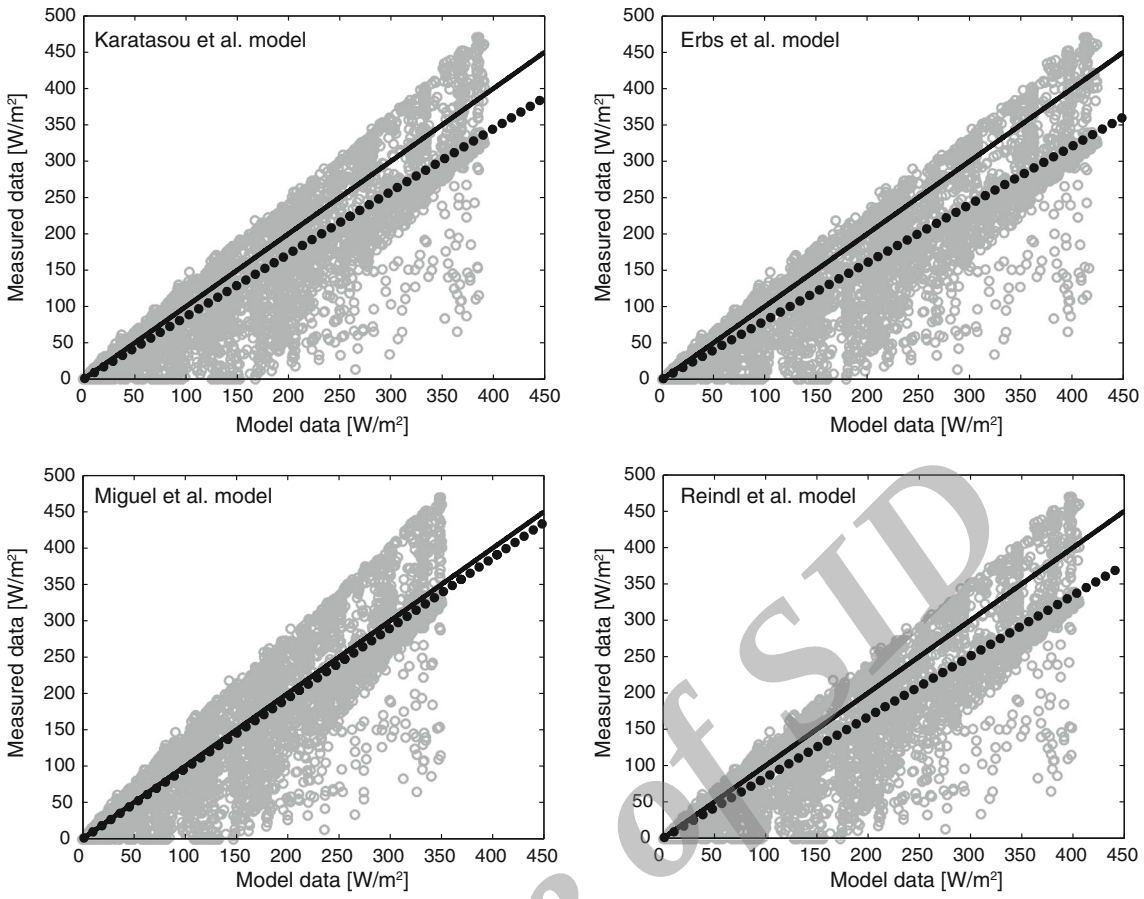

Fig. 5 Experimental versus modeled hourly values of diffuse irradiation D_h on a horizontal surface for Rome, with a linear line of best fit (*dotted line*) and a line of one-to-one correlation (*solid line*)

(solid line) for comparison purposes. Table 1a, b presents the modeled statistics for the diffuse D_h and direct B_h irradiance estimates, respectively, in comparison with the experimental data. The results indicate that all the models provide an acceptable agreement. The level of uncertainty for all the models, represented by the RMSE in W/m^2, varies between 25 and 50 W/m^2 for diffuse irradiance (33–61 average value) and between 80 and 125 W/m^2 for direct irradiance (27–43 % of the average value). With regard to model bias, the results indicate that the level and the direction of the bias, represented by the MBE in W/m^2, vary among the four models. Results show that the Miguel model achieves the best match with the experimental data as indicated by the deviation of the line of best fit from the line of one-to-one correlation and as confirmed by the higher R^2 values.

The models for converting the hourly horizontal diffuse irradiation D_h to the hourly diffuse irradiation D_{Th} on a tilted surface ("Hourly diffuse irradiation on a tilted surface") are compared in Fig. 7 where the values predicted by the four selected models are reported along with the experimental data measured on the horizontal surface. The figure shows the predicted values of the global irradiance G_{Th} on the tilted plane of the PV panels plotted against measured values. In addition, Table 1c presents the statistics for the global irradiance estimates. The results show that the Perez model gives the best estimate of the global irradiance on the tilted surface. The bias values (MBE) highlight that the four models exhibit a tendency to underestimate global irradiance values compared with the experimental data and that the four models achieve comparable values of R^2. The uncertainty (RMSE) ranges between 80 and 125 W/m^2.

The results of the four cell temperature models reported in Eqs. (24a–d) are shown in Fig. 8. The modeled results have been computed every 15 min using the experimental global irradiation measured on the surface of the PV panels, using Eq. (26) to estimate the ambient temperature and setting the wind speed v_w to the average value of the day (the weight of the wind speed in the used equations is not so high as to require a more accurate approximation). The results indicate that the third model

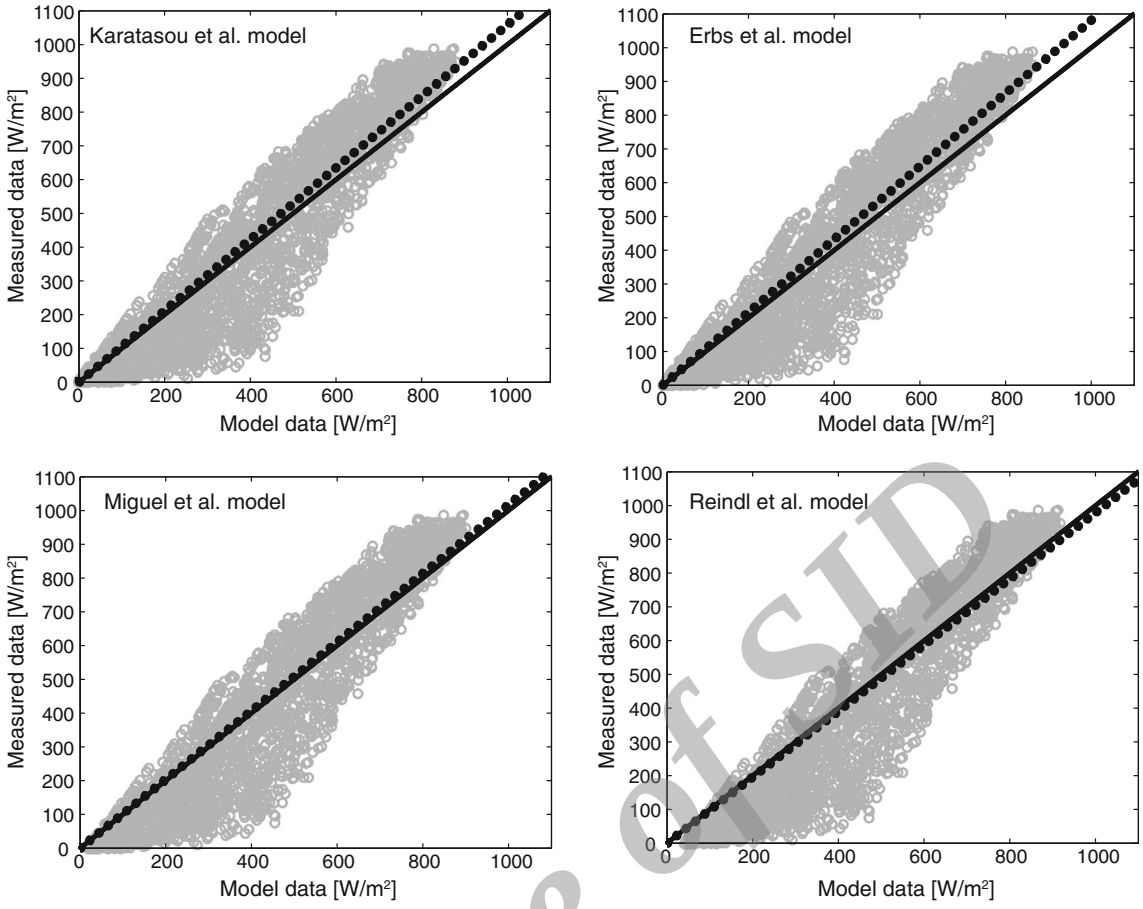

Fig. 6 Experimental versus modeled hourly values of direct irradiation B_h on a horizontal surface for Rome, with a linear line of best fit (*dotted line*) and a line of one-to-one correlation (*solid line*)

provides the closer agreement with the measured results. The level of uncertainty for all the models varies between 4 and 8 °C (23–47% of the average value) while the bias level ranges between 0.8 and 2.3 °C. The bias direction is always negative, i.e., the models tend to underestimate the cell temperature. This is mainly due to several reasons: There are uncertainties in the T_{NOCT} calculation; difficulties arise on the correct computation of the instantaneous wind velocity v_w due to the fact that there are at least seven different definitions in use as explained in [31]; the operating temperature T_c itself shows some variations in the same module and among different modules. In fact, looking at Fig. 9, which shows the temperature profiles on August 21, 2010, temperature differences of around 5 °C can be observed depending on the thermocouple position. It should be underlined that the estimation of the T_c from the back temperature T_b with reasonable accuracy is here possible because the modules are standard crystalline ones. When modules are specially designed for some particular applications, extra care must be exercised. It should be observed that a heating of the module is observed during the afternoon–evening period: This makes differences between T_c and T_a higher in the afternoon than in the morning for the same values of irradiance.

Figure 10 shows the comparison between the profiles of the ambient temperature T_a measured during two representative days and the profiles estimated through Eq. (26) starting from average historical temperature data (http://www.ilmeteo.it). It can be observed that the accuracy is reasonable; when the day is particularly clear and the irradiation is high (e.g., June 21) the measured profile rises a little faster than the predicted one. Yet, the differences remain always below 5 °C.

Model combination results

From the previous results, it was found that the Miguel model, the Perez model, and Eq. (24c) achieve the best estimates of, respectively, the diffuse irradiance on a horizontal surface, the diffuse irradiance on a tilted surface and the cell temperature. However, it is possible to

Table 1 Irradiation and temperature statistics for model estimates against measured data

Model	MBE	RMSE	R^2
(a) Hourly horizontal diffuse irradiance D_h in W/m^2			
Karatasou	+17.065	42.707	0.839
Erbs	+20.332	47.642	0.799
Miguel	+6.334	26.678	0.881
Reindl	+18.443	44.678	0.823
(b) Hourly horizontal direct irradiance B_h in W/m^2			
Karatasou	−42.459	125.004	0.820
Erbs	−21.398	80.770	0.818
Miguel	−7.54	118.221	0.902
Reindl	+35.431	96.254	0.828
(c) Hourly global irradiance G_{Th} in W/m^2			
Ma-Iqbal	−15.875	143.623	0.770
Muneer	−9.169	142.357	0.784
Perez	−0.320	137.428	0.815
Reindl	−7.581	142.219	0.792
(d) Cell temperature T_c in °C computed every 15 min			
Eq. (24a)	−2.330	3.263	0.579
Eq. (24b)	−0.978	7.349	0.645
Eq. (24c)	−0.340	4.193	0.884
Eq. (24d)	−0.530	8.005	0.820

observe, especially for the global irradiance on a tilted surface and the cell temperature, that none of the models consistently outrank the other ones. Hence, we have tried all the possible combinations of the models used for the estimation of the hourly horizontal diffuse (direct) irradiance, the hourly global irradiance on the titled surface and the cell temperature, in order to identify the best combination. Table 2 presents the statistical results for the comparison between the most significant values predicted by some combinations and the measured values for the cell temperature T_c. The statistics confirm that the combination of Miguel, Perez, and Eq. (24c) achieves the highest level of accuracy for the cell temperature.

Conclusions

The paper presents an exhaustive methodology for the estimation of the transient operating cell temperature of a PV system. The proposed procedure estimates the transient temperature of the photovoltaic cell during the day n_d of the year, placed on a surface S_T tilted γ_t from the horizontal

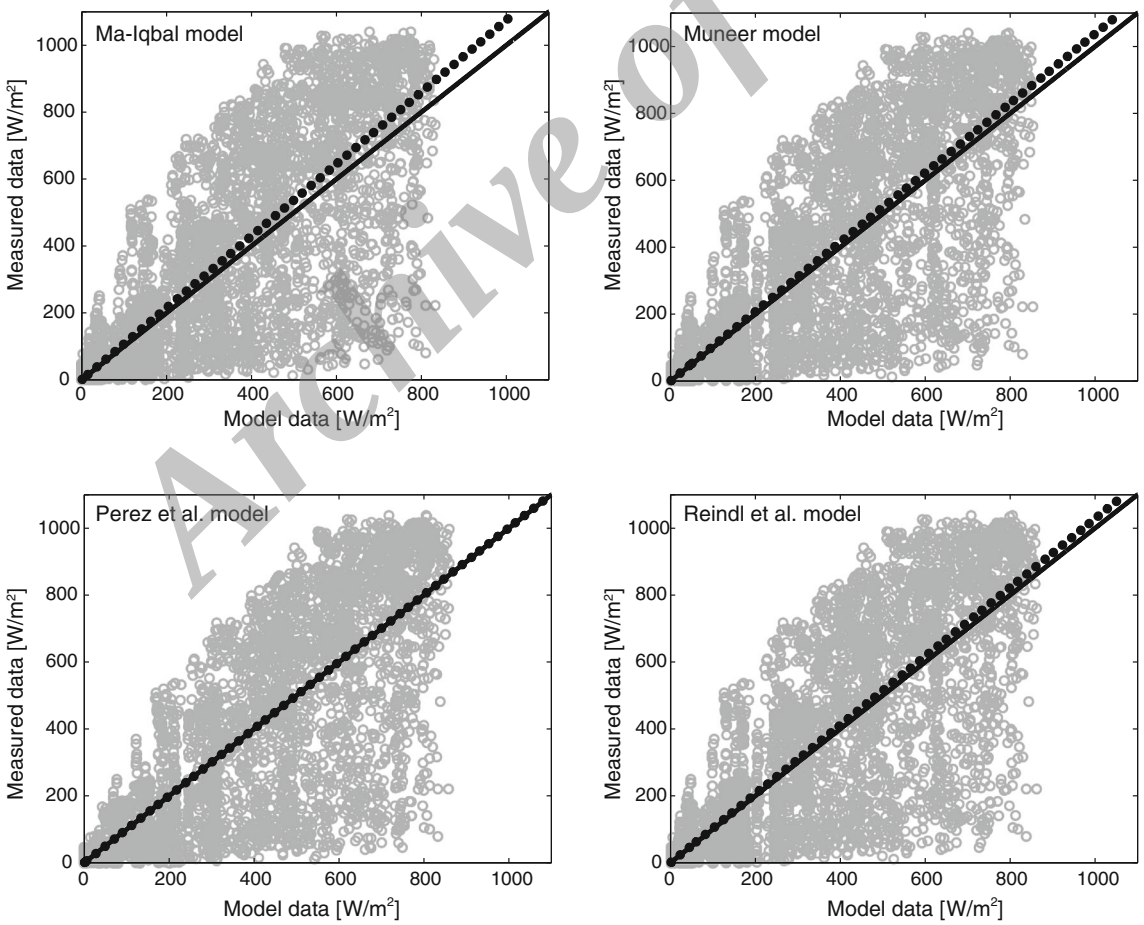

Fig. 7 Experimental versus modeled hourly values of global irradiation G_{Th} on a tilted surface for Rome, with a linear line of best fit (*dotted line*) and a line of one-to-one correlation (*solid line*)

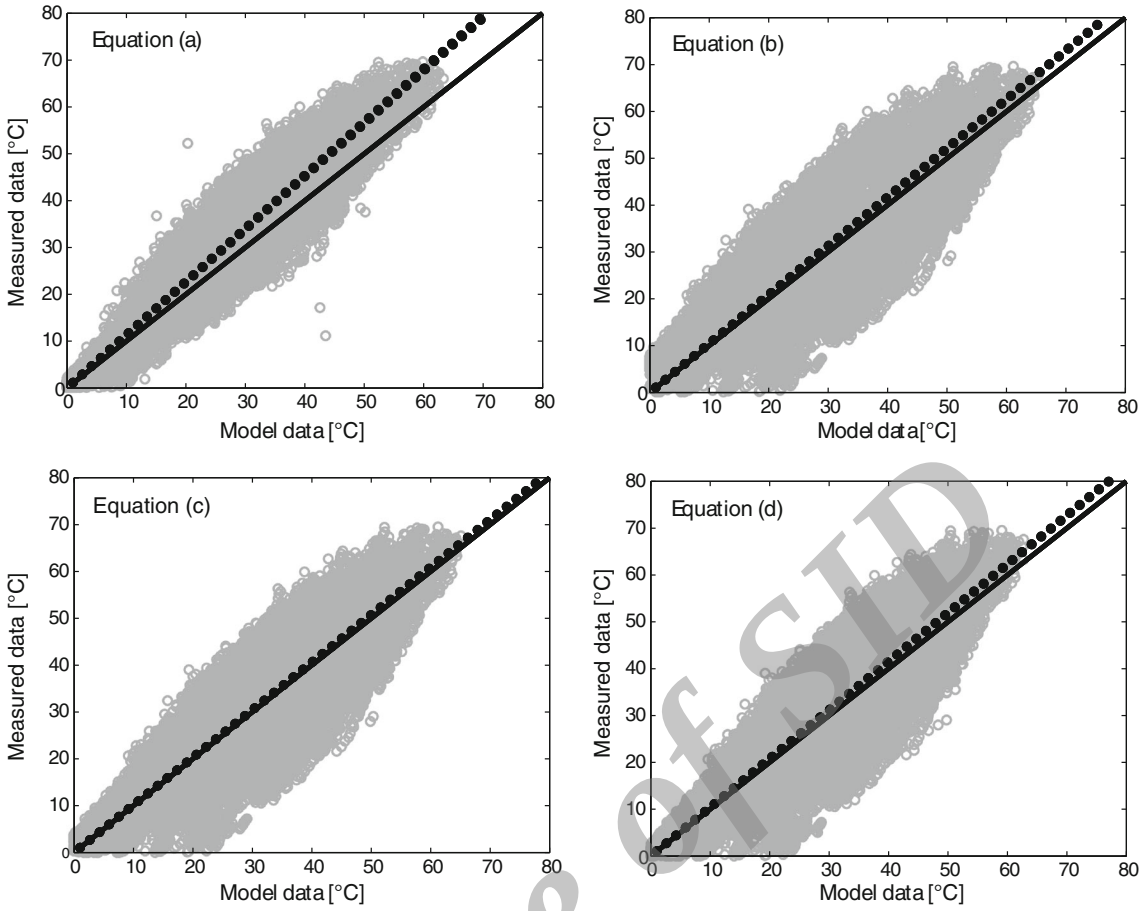

Fig. 8 Experimental versus modeled hourly values of cell temperature T_c for Rome, with a linear line of best fit (*dotted line*) and a line of one-to-one correlation (*solid line*)

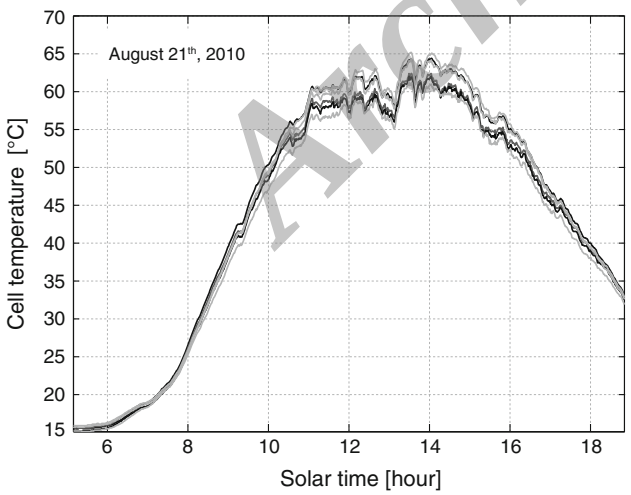

Fig. 9 Differences in module temperatures on August 21st measured by the six thermocouples

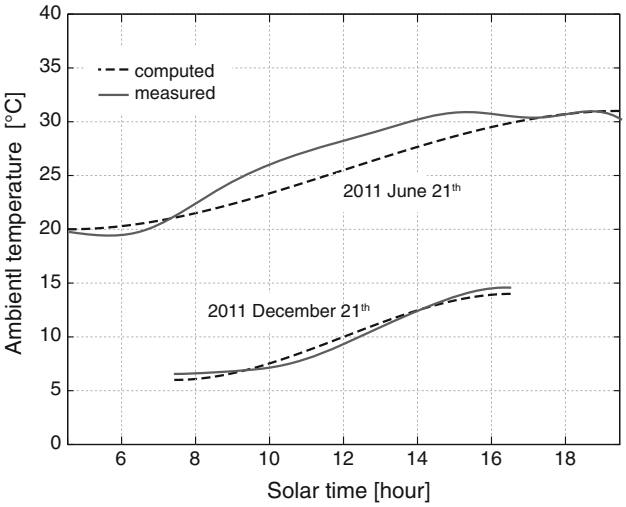

Fig. 10 Comparison between the estimated ambient temperature profile and the measured data for two representative days

Table 2 Temperature statistics for combination modeled estimates against measured data

D_h model	D_{Th} model	T_c model	MBE	RMSE	R^2
Miguel	Perez	Eq. (24c)	−0.340	4.193	0.884
Karatasou	Muneer	Eq. (24d)	−0.384	4.524	0.792
Reindl	Reindl	Eq. (24c)	+0.415	5.142	0.715
Erbs	Ma-Iqbal	Eq. (24a)	−0.854	5.836	0.693

plane and rotated α_t from the north–south direction, starting from the monthly average daily global irradiation value $\overline{H}$ on a horizontal surface. The study is considered of high interest since the values of horizontal solar irradiation are often the only data provided by meteorological stations.

The procedure consists of five steps that are applied one after another in succession:

- computation of the hourly global irradiation on a horizontal surface H_h;
- computation of the hourly diffuse irradiation on a horizontal surface D_h;
- computation of the hourly diffuse irradiation on a tilted surface D_{Th};
- computation of the irradiance time profile $I(t)$;
- computation of the cell temperature T_c.

Several well-established models have been used at each step, and the accuracy of different combinations of these models has been investigated in comparison with data measured in Rome. In addition, two new models for calculating the solar irradiance and the ambient temperature profiles have been also provided.

An error analysis, based on well-known statistical indicators, i.e., mean bias error (MBE), root mean square error (RMSE), and the coefficient of determination (R^2), reveals that the combination of Collares–Pereira, Miguel, Perez, proposed irradiation model, and Eq. (24c) achieves the highest level of model accuracy for the cell temperature. However, it has been observed that, especially as concern the global irradiance on a tilted surface and the cell temperature, none of the models consistently outrank the other ones.

Acknowledgments None.

Conflict of interest The authors declare that they have no competing interest.

Authors' contributions RA and SC developed the models; RA carried out the calculations; UG performed the measurements. All authors read and approved the final manuscript.

References

1. Rosen, M.A., Dincer, I.: On exergy and environmental impact. Int. J. Energy Res. **21**, 643–654 (1997)
2. Joshi, A.S., Dincer, I., Reddy, B.V.: Performance analysis of photovoltaic systems: a review. Renew. Sustain. Energy Rev. **13**(8), 1884–1897 (2009)
3. Dresselhaus, M.S., Thomas, I.L.: Alternative energy technologies. Nature **414**(6861), 332–7 (2001)
4. Farret, F.A., Simões, M.G.: Integration of Alternative Sources of Energy. Wiley-IEEE Press, New York (2006)
5. Eddine, B., Salah, M.: Solid waste as renewable source of energy: current and future possibility in Algeria. Int. J. Energy Environ. Eng. **3**, 17 (2012)
6. Lucchetti, E., Barbier, J., Araneo, R.: Assessment of the technical usable potential of the TUM Shaft Hydro Power plant on the Aurino River, Italy. Renew. Energy **60**, 648–654 (2013)
7. Sharma, P., Harinarayana, T.: Solar energy generation potential along national highways. Int. J. Energy Environ. Eng. **4**(16), 1–13 (2013)
8. Zahedi, A.: Solar photovoltaic (PV) energy; latest developments in the building integrated and hybrid PV systems. Renewable Energy **31**(5), 711–718 (2006)
9. Šúri, M., Huld, T.A., Dunlop, E.D., Ossenbrink, H.A.: Potential of solar electricity generation in the European Union member states and candidate countries. Sol. Energy **81**(10), 1295–1305 (2007)
10. Sharma, P., Harinarayana, T.: Enhancement of energy generation from two layer solar panels. Int. J. Energy Environ. Eng. **3**(12), 1–9 (2012)
11. Jäger-Waldau, A., Szabó, M., Scarlat, N., Monforti-Ferrario, F.: Renewable electricity in Europe. Renew. Sustain. Energy Rev. **15**(8), 3703–3716 (2011)
12. Kolhe, M.: Techno-economic optimum sizing of a stand-alone solar photovoltaic system **24**(2):511–519 (2009)
13. Notton, G., Lazarov, V., Stoyanov, L.: Optimal sizing of a grid-connected PV system for various PV module technologies and inclinations, inverter efficiency characteristics and locations. Renew. Energy **35**(2), 541–554 (2010)
14. Grasselli, U.: Probabilistic design of high quality power supply photovoltaic systems. In Proceedings of IEEE-IAS I&CPS May 2–6, St Petersburg, Florida, USA (1993)
15. Grasselli, U.: A probabilistic method for simulation and design optimization of stand-alone photovoltaic systems. In Proceedings of UPEC September 18–20, Iraklio, Crete, Greece (1996)
16. Araneo, R., Lammens, S., Grossi, M., Bertone, S.: EMC issues in high-power grid-connected photovoltaic plants. IEEE Trans. Electromag. Compat. **51**, 639–648 (2009)
17. Notton, G., Cristofari, C., Poggi, P., Muselli, M.: Calculation of solar irradiance profiles from hourly data to simulate energy systems behaviour. Renew. Energy **27**, 123–142 (2002)
18. Eltawil, M.A., Zhao, Z.: Grid-connected photovoltaic power systems: Technical and potential problems—a review. Renew. Sustain. Energy Rev. **14**, 112–129 (2010)
19. Kim, S.K., Jeon, J.H., Cho, C.H., Kim, E.S., Ahn, J.B.: Modeling and simulation of a grid-connected PV generation system for electromagnetic transient analysis. Sol. Energy **83**(5), 664–678 (2009)
20. Femia, N., Lisi, G., Petrone, G., Spagnuolo, G., Vitelli, M.: Distributed maximum power point tracking of photovoltaic arrays: novel approach and system analysis. IEEE Trans **55**(7), 2610–2621 (2008)
21. Nordmann, T., Clavadetscher, L.: Understanding temperature effects on PV system performance. In Proceedings of 3rd World Conference on Photovoltaic Energy Conversion 3:2243–2246 (2003)

22. King, D.L., Kratochvil, J.A., Boyson, W.E.: Temperature coefficients for PV modules and arrays : Measurement methods, difficulties, and results. In 26th IEEE Photovoltaic Specialists Conference (1997)
23. Skoplaki, E., Palyvos, J.: On the temperature dependence of photovoltaic module electrical performance: A review of efficiency/power correlations. Sol. Energy **83**(5), 614–624 (2009)
24. Wysocki, J.J.: Effect of temperature on photovoltaic solar energy conversion. J. Appl. Phys. **31**(3), 571–578 (1960)
25. Lasnier, F., Gang-Ang, T.: Photovoltaic Engineering Handbook. Adam Hilger, Bristol (1990)
26. Messenger, R.A., Ventre, J.: Photovoltaic Systems Engineering. CRC Press/Taylor & Francis (2010)
27. Solanki, C.S.: Solar Photovoltaics: Fundamentals, Technologies and Applications. Prentice-Hall of India Pvt. Ltd. (2011)
28. Ferguson, L.G., Fraasb, L.M.: Theoretical study of GaSb PV cell efficiency as a function of temperature. Sol. Energy Mater. Sol. Cells **39**, 11–18 (1995)
29. Araneo, R., Falconi, C.: Lateral bending of tapered piezosemiconductive nanostructures for ultra-sensitive mechanical force to voltage conversion.. Nanotechnology **24**(26), 265707 (2013)
30. Araneo, R., Lovat, G., Burghignoli, P., Falconi, C.: Piezo-semiconductive quasi-1D nanodevices with or without anti-symmetry. Adv. Mater (Deerfield Beach, Fla.) **24**(34), 4719–24 (2012)
31. Skoplaki, E., Boudouvis, A.G., Palyvos, J.A.: A simple correlation for the operating temperature of photovoltaic modules of arbitrary mounting. Solar Energy Mater Solar Cells **92**, 1393–1402 (2008)
32. Skoplaski, E., Palyvos, J.A.: Operating temperature of photovoltaic modules: a survey of pertinent correlations. Renew. Energy **34**, 23–29 (2009)
33. Duffie, J.A., Beckman, W.A.: Solar engineering of thermal processes. Wiley, 3rd edition, New York (2006)
34. Li, H., Bu, X., Lian, Y., Zhao, L., Ma, W.: Further investigation of empirically derived models with multiple predictors in estimating monthly average daily diffuse solar radiation over China. Renew. Energy **44**, 469–473 (2012)
35. Mubiru, J., Banda, E.: Monthly average daily global solar irradiation maps for Uganda: A location in the equatorial region. Renew. Energy **41**, 412–415 (2012)
36. Muneer, T.: Solar Radiation and Daylight Models. Butterworth-Heinemann Ltd (2004)
37. Moharil, R.M., Kulkarni, P.S.: Reliability analysis of solar photovoltaic system using hourly mean solar radiation data. Sol Energy **84**, 691–702 (2010)
38. Page, J.K.: New sources of energy. In Proceedings of United Nations Conference on New Sources of Energy, Solar Energy, Wind Power and Geothermal Energy **4**:378 (1961)
39. Liu, B.Y.H., Jordan, R.C.: The interrelationship and characteristic distribution of direct, diffuse and total solar insolation. Sol Energy **1**, 1–19 (1960)
40. Jain, P.C.: Comparison of techniques for the estimation of daily global irradiation and a new technique for the estimation of hourly global irradiation. Solar Wind Technol **1**, 123–134 (1988)
41. Collares-Pereira, M., Rabl, A.: The average distribution of solar radiation-correlations between diffuse and hemispherical and between daily and hourly insolations values. Sol Energy **22**, 155–164 (1979)
42. Iqbal, M.: A study of Canadian diffuse and total solar radiation data, II. Monthly average hourly horizontal radiation. Sol Energy **22**, 87–90 (1979)
43. Jain, P.C., Jain, S., Ratto, C.F.: A new model for obtaining horizontal instantaneous global and diffuse radiation from the daily values. Sol Energy **41**, 397–404 (1988)
44. Wu, J., Chan, C.K.: Prediction of hourly solar radiation using a novel hybrid model of ARMA and TDNN. Sol Energy **85**, 808–817 (2011)
45. Hocaoğlu, F.O., Gerek, O.N., Kurban, M.: Hourly solar radiation forecasting using optimal coefficient 2-D linear filters and feed-forward neural networks. Sol Energy **82**, 714–726 (2008)
46. Notton, G., Muselli, M., Louche, A.: Two estimation methods for monthly mean hourly total irradiation on tilted surfaces from monthly mean daily horizontal irradiation from solar radiation data of Ajaccio, Corsica. Sol Energy **57**, 141–153 (1996)
47. Jacovideis, C.P., Tymvios, F.S., Assimakopoulos, V.D., Kaltsounides, N.A.: Comparative study of various correlations in estimating hourly diffuse fraction of global solar irradiation. Renew. Energy **31**, 2492–2504 (2006)
48. Mondol, J.D., Yohanis, Y.G., Norton, B.: Solar radiation modelling for the simulation of photovoltaic systems. Renew. Energy **33**, 1109–1120 (2008)
49. Jacovides, C.P., Boland, J., Asimakopoulos, D.N., Kaltsounides, N.A.: Comparing diffuse radiation models with one predictor for partitioning incident PAR radiation into its diffuse component in the eastern Mediterranean basis. Renew. Energy **35**, 1820–1827 (2010)
50. Karatasou, S., Santamouris, M., Geros, V.: Analysis of experimental data on diffuse solar radiation in Athens, Greece for building application. Int. J. Sustain. Energy **23**, 1–11 (2003)
51. Erbs, D.G., Klein, S.A., Duffie, J.A.: Estimation of the diffuse radiation fraction for hourly, daily and monthly average global radiation. Sol Energy **28**, 293–302 (1982)
52. Miguel, A., Bilbao, J., Aguiar, R., Kambezidis, H., Negro, E.: Diffuse solar radiation model evaluation in the north Mediterranean belt area. Sol Energy **70**, 143–153 (2001)
53. Reindl, D.T., Beckman, W.A., Duffie, J.A.: Diffuse fraction correlations. Sol Energy **45**, 1–7 (1990)
54. Iqbal M (1983) An introduction to solar radiation. New York: Academic
55. Noorian, A.M., Morandi, I., Kamali, G.A.: Evaluation of 12 models to estimate hourly diffuse irradiation on inclined surfaces. Renew. Energy **33**, 1406–1412 (2008)
56. Evseev, E.G., Kudish, A.I.: The assessment of different models to predict the global solar radiation on a surface tilted to the South. Sol Energy **83**, 377–388 (2009)
57. Loutzenhiser, P.G., Manz, H., Felsmann, C., Strachan, P.A., Frank, T., Maxwell, G.: Empirical validation of models to compute solar irradiance on inclined surfaces for building energy simulation. Sol Energy **81**, 254–267 (2007)
58. Ma, C.Y., Iqbal, M.: Statistical comparison of models for estimating solar radiation on inclined surfaces. Sol Energy **31**, 313–317 (1983)
59. Reindl, D.T., Beckman, W.A., Duffie, J.A.: Evaluation of hourly tilted surface radiation models. Sol Energy **45**, 9–17 (1990)
60. Muneer T (1997) Solar Radiation and Daylight Models for the Energy Efficient Design of Buildings. Oxford: Architectural Press
61. Perez, R., Stewart, R., Arbogast, R., Seals, J., Scott, J.: An anisotropic hourly diffuse radiation model for surfaces: description, performance validation, site dependency evaluation. Sol Energy **36**, 487–497 (1986)
62. Perez, R., Ineichen, P., Seals, R., Michalsky, J.J., Stewart, R.: Modelling daylight availability and irradiance components from direct and global irradiance. Sol Energy **44**, 271–289 (1990)
63. Hay, J.E.: Study of shortwave radiation on non-horizontal surfaces. Tech. Rep. 79–12, Atmospheric Environment Service, Downsview, Ontario (1979)
64. Temps, R.C., Coulson, K.L.: Solar radiation incident upon slopes of different orientation. Sol. Energy **19**, 179–184 (1977)
65. Gueymard, C.: An anisotropic solar irradiance model for tilted surfaces and its comparison with selected engineering algorithms. Sol Energy **38**, 367–386 (1987)

66. Markvart, T.: Solar electricity. Chichester, Wiley (2000)
67. Chenni, R., Makhlouf, M., Kerbache, T., Bouzid, A.: A detailed modelling method for photovoltaic cells. Energy **32**, 1724–1730 (2007)
68. King, D., Boyson, W., Kratochvil, J.: Photovoltaic array performance model. Tech. rep., SAND2004-3535, /http://www.sandia.gov/pv/docs/PDF/King%20SANDS.pdf (2004)
69. Joint Committee for Guides in Metrology (2008) JCGM 100: Evaluation of measurement data—guide to the expression of uncertainty in measurement. BIPM-Bureau International des Poids et Mesures